Mechanical Design of the LMF Target Chamber

R.L. Engelstad, J.W. Powers and E.G. Lovell

October 1990

UWFDM-828

Presented at the 9th Topical Meeting on the Technology of Fusion Energy, 7–11 October 1990, Oak Brook IL.

FUSION TECHNOLOGY INSTITUTE

UNIVERSITY OF WISCONSIN

MADISON WISCONSIN

Mechanical Design of the LMF Target Chamber

R.L. Engelstad, J.W. Powers and E.G. Lovell

Fusion Technology Institute
University of Wisconsin
1500 Engineering Drive
Madison, WI 53706

http://fti.neep.wisc.edu

October 1990

UWFDM-828

Presented at the 9th Topical Meeting on the Technology of Fusion Energy, 7–11 October 1990, Oak Brook IL.

MECHANICAL DESIGN OF THE LMF TARGET CHAMBER

R.L. Engelstad, J.W. Powers, E.G. Lovell
Fusion Technology Institute
University of Wisconsin-Madison
1500 Johnson Drive
Madison, WI 53706
(608) 262-5745

ABSTRACT

Results are presented for the preliminary mechanical design of a light ion beam Laboratory Microfusion Facility (LMF). Applications of the facility include the development of high gain, high yield ICF targets. The LMF target chamber must meet the requirements imposed by the ion beam propagation, and survive severe target blast loadings. Yields from 10 to 1000 MJ are considered for a projected lifetime of up to 15,000 shots. The chamber will be subjected to repeated loadings that include intense x-ray vaporization of the first wall surface, resulting in large amplitude pressure waves. A carbon/carbon composite thermal liner has been proposed to attenuate the radial shock waves and protect the structural wall. Nevertheless, the chamber wall must still be designed to withstand large impulsive and residual pressures. The proposed target chamber consists of a capped cylindrical shell that is 1.5 m in radius and 4.5 m in height. The analysis of the mechanical response of the structural wall from the repetitive dynamic overpressures is described in detail. Modified elastic constants are used to account for the higher ligament stresses and strains which are present between the beam ports and diagnostic ports. In addition, fatigue lifetime calculations have been made according to ASME guidelines, applying cumulative damage criteria specified by Miner's rule. A modified rainflow cycle counting method was used in conjunction with Goodman diagrams to determine equivalent stresses and strains to be used with the constant amplitude, fully reversed fatigue data. Both 6061-T6 aluminum and 2 1/4 Cr - 1 Mo steel are considered for the structural materials, with maximum stress and fatigue design results developed for a range of thicknesses and overpressures.

INTRODUCTION

A research program has been developed by Sandia National Laboratories (SNL) and the UW Fusion Technology Institute to support the initial design of a light ion beam LMF. This effort includes a mechanical analysis of critical aspects of the chamber to identify sizes, compare response of structural materials and establish basic design characteristics. The relative features of the target chamber, water shield and beam lines are shown in Figure 1, and the chamber's principal mechanical parameters are listed in Table 1. For practical reasons related to fabrication experience and cost, the base case is a capped cylindrical pressure vessel. It can be seen from Figure 2 that the shell is highly perforated, requiring an assessment of reduced stiffness and increased stress in these regions.

Table 1. Mechanical Parameters for the LMF Chamber.

Geometry	Capped Cylindrical Shell
Radius	1.5 m
Cylindrical Wall Height	4.5 m
Number of Beam Ports	36
Port Diameters	36 cm
Fill Gas	10 torr He
Thermal Liner Thickness	2 cm
Thermal Liner Material	Carbon/carbon composite
Structural Material	Al 6061-T6, or 2 1/4 Cr - 1 Mo Steel

The aluminum alloys are considered in order to minimize the radiological dose near the chamber during the initial period after operation. The 2 1/4 Cr - 1 Mo steel is a candidate material because it has been widely used in conventional nuclear installations and thus has well documented characteristics. Basic mechanical properties of these alloys can be found in Table 2.

Table 2. Static Properties of Chamber Materials.[1,2]

	Aluminum 6061 - T6	Steel 2 1/4 Cr - 1 Mo
Yield Strength	103 MPa	206 MPa
Ultimate Strength	166 MPa	415 MPa
Elastic Modulus	68.9 GPa	216 GPa
Poisson's Ratio	0.33	0.26
Mass Density	2710 kg/m^3	7825 kg/m^3

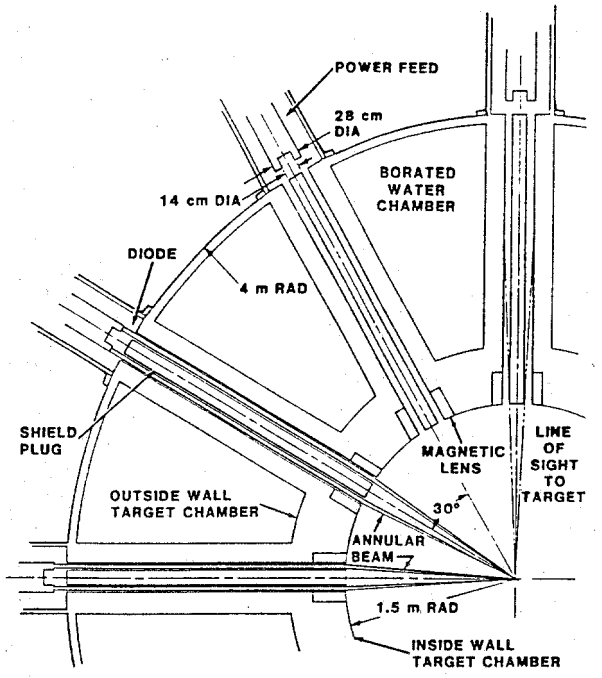

Figure 1. Plan view of target chamber, water shield and beam lines.

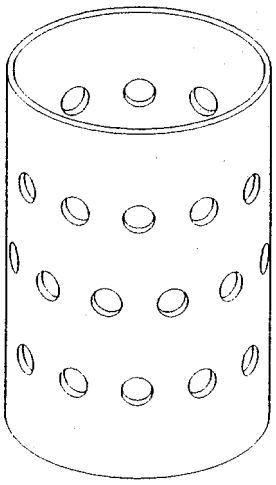

Figure 2. Chamber cylindrical shell showing beam ports.

The structural wall is protected from the intense thermal load and target debris by a liner of carbon/carbon composite. Compared with traditional graphites, such composites have higher resistance to crack growth and a reduced solid density which better accommodates transient thermal strains. Weaves with fibers through the thickness raise delamination thresholds from shock and in addition the composites can be fabricated into complex configurations. Additional features of the LMF design are described in a more general overview paper by Ramirez et al.[3]

The LMF target chamber will be subjected to blast loadings with target yields ranging from 10 to 1000 MJ. These pressure loads consist of two components: an initial pressure spike caused by the rapid x-ray vaporization of the first wall surface and a residual afterpressure due to the resulting energy content of the vapor and the target chamber gas. The hydrodynamics code CONRAD[4] was used to calculate the initial pressure loading. For example, Figure 3 shows a load history for a 1000 MJ target yield where the duration of the initial spike is on the order of a few nanoseconds. Thus, when compared with the response time of the shell (or the natural period of vibration), the loading can be characterized by an impulse. Consequently, the dynamic response will depend upon the magnitude of the impulse but it will be insensitive to the shape of the pressure spike. In addition to this initial impulse, a steady afterpressure of a sizable amount follows. Table 3 shows the pressure loadings considered in this analysis for various target yields. The residual pressures, also referred to as $P_{static,}$ were computed from $(\gamma\text{-}1)E/V$ where γ is the ratio of specific heats for the gas, E is the thermal energy in the gas and V is the gas volume. Additional details on the hydrodynamic calculations and formulations for the LMF design can be found in a companion paper by Peterson.[5]

Table 3. Pressure Loadings on the LMF Chamber.

Target Yield (MJ)	Impulsive Pressure (Pa-s)	Residual Pressure P_{static} (MPa)
1000	284	0.77
200	55	0.22
50	10	0.062
10	0.7	0.0062

Since the exact rise time of the residual pressure is unknown, the loading function has been modeled as a dynamic step function, which is actually more severe. This step load is superimposed with the impulse load to provide a complete load versus time history for the LMF chamber wall (see Figure 4).

DYNAMIC RESPONSE OF THE CHAMBER

The pressure loads are assumed to be uniformly distributed over the wall of the chamber, resulting in an axisymmetric mechanical response that is also symmetric with respect to the midspan plane. If the chamber is assumed to be rigidly supported at the ends, the largest stresses in the cylinder (due to bending) will occur near these supports. However, by increasing the wall thickness in these areas, localized stresses can be controlled. Thus, the basis for the design is the circumferential normal stress

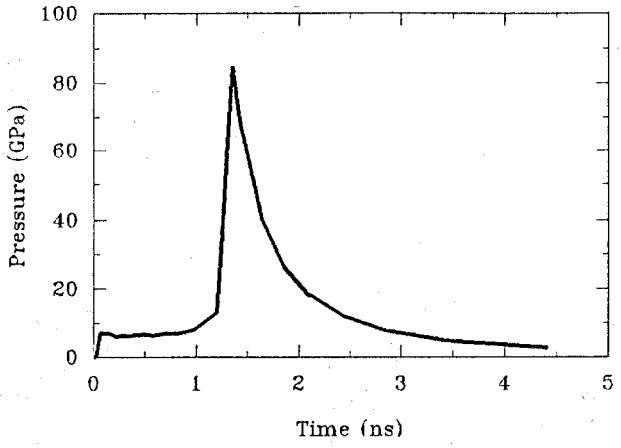

Figure 3. Pressure history at 1.5 m radius chamber wall for 1000 MJ yield.

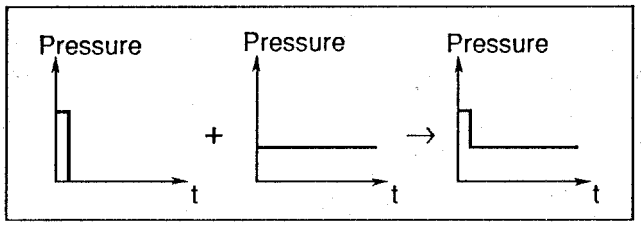

Figure 4. Superposition of impulse and step pressure.

that is present at the midspan. It is also assumed that the longitudinal (or axial) stress will be zero at this location resulting in a uniaxial state of stress.

In order to account for the weakening effect of the shell perforations on the mechanical response of the chamber's wall, modified effective elastic constants are used in place of actual material properties. These equivalent efficiency factors have been successfully used for years in the design of perforated tube-sheets and tube-plates.[6-8] The method has been extended to the research here with the intent of determining an equivalent solid cylinder that can be analyzed by conventional shell equations. Two types of perforation patterns have been considered, i.e., triangular and square. These are shown in Figure 5 with the pitch P defined as the distance between perforation centers and the ligament efficiency μ defined as 1.0 - d/P where d is the diameter of the perforation. With the numerical data for specific geometries being somewhat limited, ligament efficiencies of 0.33 and 0.40 have been used for the triangular and square perforation patterns, respectively. For the configuration and geometry of the LMF chamber, μ is actually 0.54. Thus the design is again on the conservative side. In fact with the lower ligament efficiencies used in the calculations, the design is comparable to a chamber with up to 15 beam ports (36 cm in diameter) in each of the 3 tiers, instead of the proposed 12 (see Figure 2). Figures 6 and 7 show the data used for both the elastic modulus E* and Poisson's ratio ν*, as a function of the wall thickness, h.[6] It is these curves which

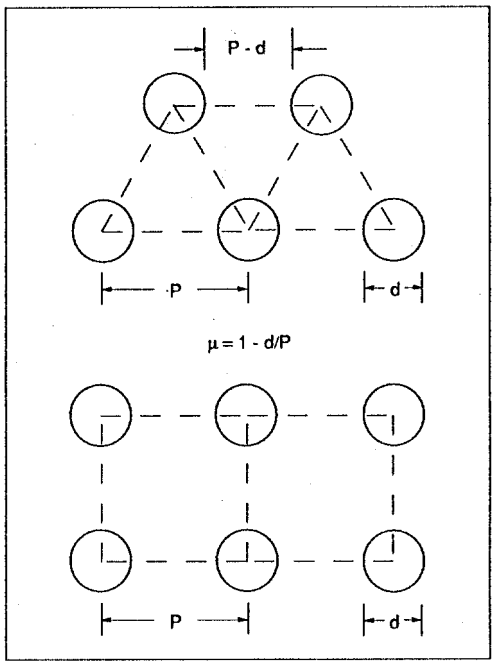

Figure 5. Wall perforation patterns.

are programmed into the structural response and fatigue code.

With the effective elastic constants known, the mechanical response of the shell can be computed. For example, Figure 8 gives the circumferential stress history for an aluminum chamber with a square perforation pattern and a thickness of 13.0 cm. The loading in this case is only the short-duration impulsive pressure (284 Pa-s) corresponding to the 1000 MJ target. On the contrary, Figure 9 shows the effect of a dynamic step load equivalent to P_{static} (0.77 MPa) superimposed on the impulse load. Obviously, the initial transient stress has virtually doubled in magnitude, and the steady-state response is damping out to the equivalent value of the static stress due to the afterpressure. Consequently, what may seem like a relatively insignificant residual pressure, may actually produce a substantial mean stress in addition to amplifying the alternating stress. It is essential then to consider the mechanical stress history from both the short duration impulse loading and the long duration afterpressure in the fatigue calculations. Additionally, corresponding strain histories are determined by again employing the effective elastic constants.

CHAMBER LIFETIME ANALYSIS

Cumulative damage is used in the fatigue analysis since each stress/strain history is characterized by cycles of different amplitude and each target yield will produce a different history. Because of the mean stresses/strains present in addition to the alternating stresses/strains, an appropriate cycle counting method is used to determine an

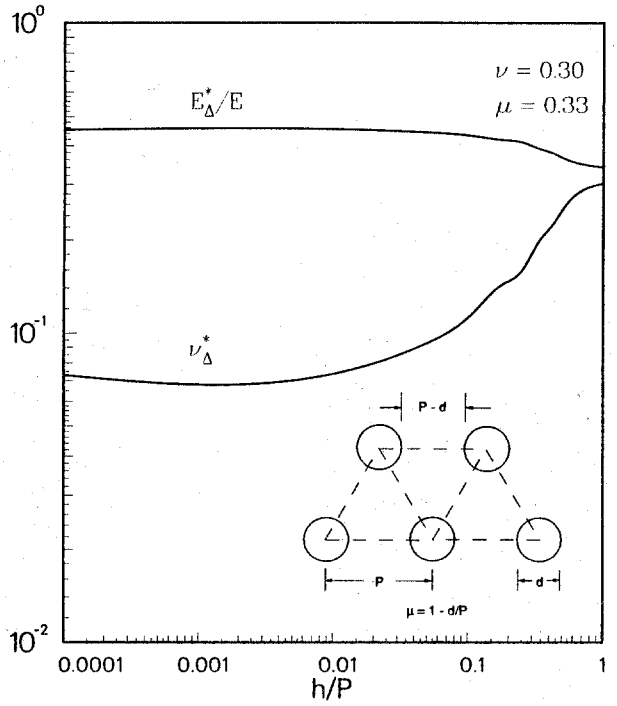

Figure 6. Effective elastic constants for a triangular perforation pattern.

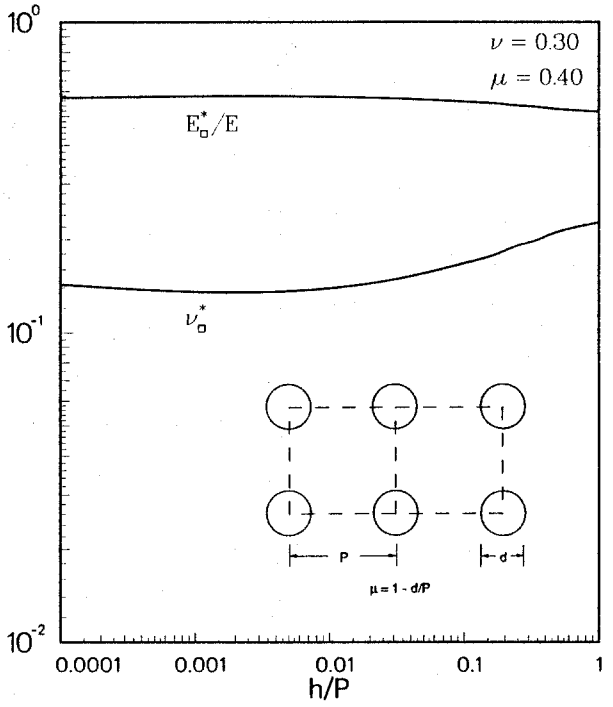

Figure 7. Effective elastic constants for a square perforation pattern.

equivalent history that can be evaluated with the constant amplitude, fully reversed fatigue data. One of the most widely accepted techniques, and one of the most accurate, is the rainflow method. The algorithm used to perform the rainflow cycle counting has been taken from the recommended procedures published by the American Society of Testing and Materials (ASTM).[9] A Goodman diagram is used in conjunction with the cycle counting in order to obtain the value of the equivalent range stress/strain. Finally, Miner's rule is applied to estimate the linear, cumulative damage effects. This failure criterion can be expressed as

$$\sum_{j=1} (n/N_f)_j \leq D$$

where n is the number of applied cycles of loading conditions j, N_f is the number of design allowable cycles of the loading conditions and D is the allowable damage limit. Thus, failure is predicted if the total damage is greater or equal to 1.0.

It should be noted that the procedure outlined above (for the fatigue lifetime calculations) is consistent with the intent and methodology of the ASME Pressure Vessel Code.[10,11] Safety factors of either two on stress/strain or twenty on cycles is specified by the code; however, for the type of loading conditions on the LMF chamber, a factor of safety of two is more conservative.

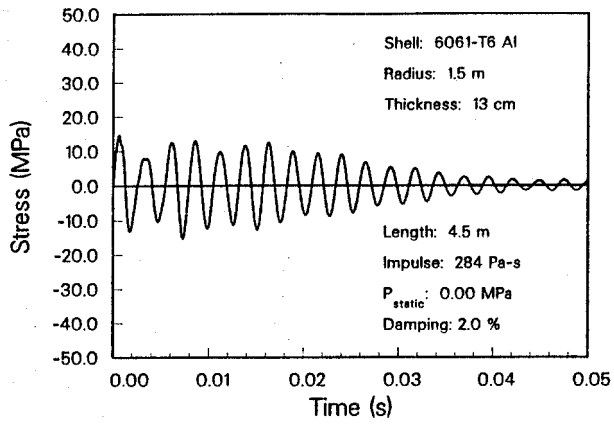

Figure 8. Circumferential mechanical stress from impulsive loading alone.

Two materials were considered in the structural analysis of the LMF chamber, 2 1/4 Cr-1 Mo steel and 6061-T6 aluminum. Figure 10 shows the strain-based fatigue data for 2 1/4 Cr-1 Mo that were published by Booker et al., at ORNL.[12] The data were obtained from completely reversed loadings with constant amplitude strains applied at the rate of 4×10^{-1}/s. The latest fatigue data on welded Al 6061-T6 was obtained from the Aluminum Association and is shown in Figure 11.[1,13] The data (stress-based) were given for "Category B" type welded joints. The lower 95% confidence limit, as shown on the curve, has been used in all fatigue calculations. In

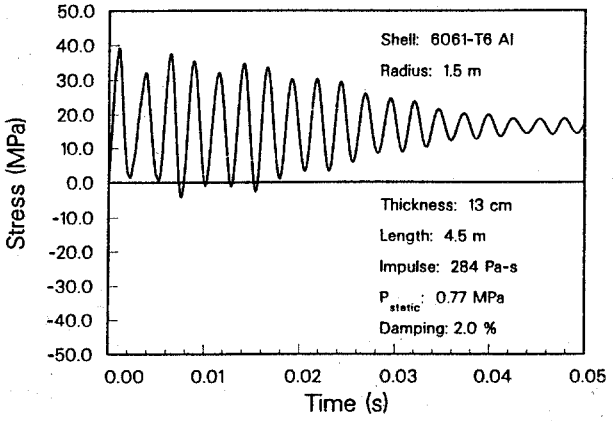

Figure 9. Circumferential mechanical stress from impulsive and static pressure.

addition, the Aluminum Association recommends that the maximum range stress should not exceed 12.0 ksi (82.8 MPa).

Fatigue calculations were carried out for lifetimes of 3, 6, 9, 12 and 30 years. Table 4 shows the cumulative shots for each of the target yields considered. The pressure loading on the chamber for each yield consists of the "Impulsive Pressure" and the "Residual Pressure" from Table 3. In addition, both the triangular and the square perforation patterns were evaluated. Table 5 gives the minimum wall thickness needed for the steel, with the corresponding results for aluminum given in Table 6.

The results of the fatigue calculations were governed by the loadings of the 1000 MJ shots for both the steel and the aluminum, with the primary failure mode being yielding. Thus the value of the thickness remains the same for lifetimes of 6, 9, 12 and 30. However, with no 1000 MJ shots present in the first 3 years, the value of the minimum thickness drops significantly. It should also be noted that the results of the fatigue calculations with steel show that the chamber can be built with a thickness of 2.4 cm or less. Since buckling becomes an issue for very thin walls, the lower limit for chamber thickness is taken as 3.0 cm.

Table 4. LMF Cumulative Shots.

Lifetime Years	Target Yield 10 MJ	50 MJ	200 MJ	1000 MJ
3	990	480	30	0
6	1800	1080	90	30
9	1950	2130	330	90
12	2010	2970	810	210
30	2190	5490	5850	1470

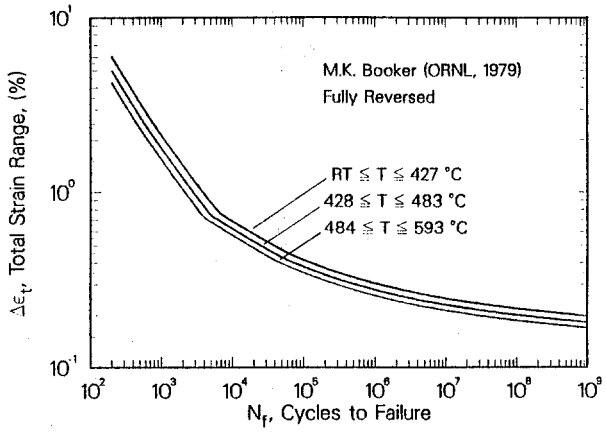

Figure 10. Fatigue data for 2 1/4 Cr - 1 Mo steel.

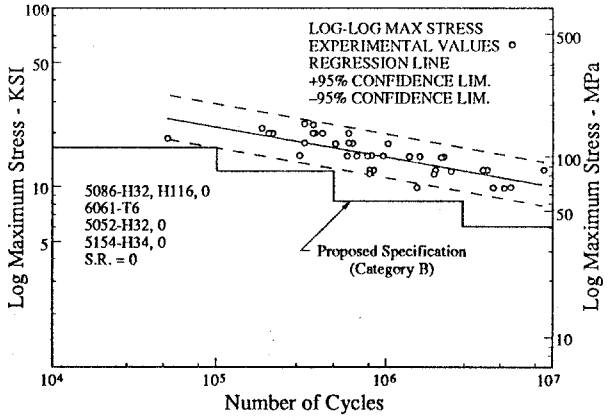

Figure 11. Fatigue data for welded 6061-T6 aluminum.

Table 5. Chamber Lifetimes for 2 1/4 Cr - 1 Mo Steel.

Triangular Perforation Patterns	
Lifetime Years	Minimum Wall Thickness
3	0.6 cm*
6,9,12,30	2.4 cm*
Square Perforation Patterns	
Lifetime Years	Minimum Wall Thickness
3	0.5 cm*
6,9,12,30	1.8 cm*

*Thickness of 3.0 cm is recommended.

Triangular Perforation Patterns

Lifetime Years	Minimum Wall Thickness
3	4.0 cm
6,9,12,30	>15.0 cm

Square Perforation Patterns

Lifetime Years	Minimum Wall Thickness
3	3.0 cm
6,9,12,30	13.0 cm

CONCLUSIONS

Mechanical analyses have been carried out for cylindrical reaction chambers of the proposed SNL light ion beam laboratory microfusion facility. Codes were developed to determine the vessel's dynamic response from impulsive and steady pressures due to target blast loadings. An assessment was made of the increase in stress and decrease in stiffness from 36 beam ports in a 1.5 m radius chamber. Wall thicknesses were established by cumulative damage fatigue criteria. This included modified rainflow cycle counting and Goodman diagrams to determine equivalent stresses and strains. Target yields from 10 MJ to 1000 MJ were included in a program totaling 15,000 shots. For 2 1/4 Cr - 1 Mo steel, the lifetime can be achieved with a wall thickness of 3.0 cm. Under the same circumstances, chambers of 6061-T6 aluminum need to be at least 13.0 cm thick. It is also shown that even a small number of high yield (1000 MJ) shots has a major influence on the size because of inelastic straining. Thus significantly thinner chambers can be designed to sustain yields of 200 MJ or less.

ACKNOWLEDGEMENT

Support for this research has been provided by the U.S. Department of Energy through Sandia National Laboratories.

REFERENCES

1. Engineering and Design Task Force, "Specifications for Aluminum Structures," Aluminum Construction Manual, Fifth Edition, The Aluminum Association, Washington, DC (1986).

2. ASTM Committee A-1 on Steel, "Standard Specification for Pressure Vessel Plates, Alloy Steel, Chromium-Molybdenum," Designation A 387/A387M-89, 1990 Annual Book of ASTM Standards, American Society for Testing and Materials, Easton, MD , 1.04, 257 (1990).

4. R.R. PETERSON, J.J. MacFARLANE AND G.A. MOSES, "CONRAD - A Combined Hydrodynamics-Condensation/Vaporization Computer Code," UWFDM-670, University of Wisconsin Fusion Technology Institute Report (1988).

5. R.R. PETERSON, "Pressure Loadings on the Walls of a Light Ion Laboratory Microfusion Facility Target Chamber," these proceedings.

6. F. OSWEILLER, "Evolution and Synthesis of the Elastic Constants, Concept from 1948 to Present - New Design Curves for Triangular and Square Patterns," Design and Analysis of Piping, Pressure Vessels, and Components, Proceedings of the 1987 Pressure Vessels and Piping Conference, 120, 137 (1987).

7. P. MEIJERS, "Refined Theory for Bending and Torsion of Perforated Plates," Pressure Vessel Components Design and Analysis, Proceedings of the 1985 Pressure Vessels and Piping Conference, 98, 11 (1985).

8. W.J. O'DONNELL, "Perforated Plates and Shells," Pressure Vessels and Piping: Design and Analysis a Decade of Progress, ASME, New York, NY (1972).

9. ASTM Committee E-9 on Fatigue, "Standard Practices for Cycle Counting in Fatigue Analysis," 1988 Annual Book of ASTM Standards, Designation: E 1049-85, American Society for Testing and Materials, 3.01, 764 (1990).

10. ASME Boiler and Pressure Vessel Code, Section III, Nuclear Power Plant Components (1986).

11. ASME Boiler and Pressure Vessel Code, Case Interpretations, Code Case N-47 (1974).

12. M.K. BOOKER, J.P. STRIZAK and C.R. BRINKMAN, "Analysis of the Continuous Cycling Fatigue Behavior of 2.25 Cr-1 Mo Steel," Oak Ridge National Laboratory Report ORNL-5593, Oak Ridge, TN (1979).

13. W.W. SANDERS, Jr. and J.W. FISHER, "Development of Recommended Specifications for Fatigue Design of Aluminum Structures," submitted to the Aluminum Association (1985).